ACADEMIA JOURNAL OF BIOLOGY 2025, 47(1): 121–135
DOI: 10.15625/2615-9023/21232

ROLE OF YEAST *HAP4* GENE IN MITOCHONDRIAL FUNCTION, OXIDATIVE PHOSPHORYLATION, AND APOPTOSIS IN RESPONSE TO DNA DAMAGE

Bui Van Ngoc[1,2,*], Nguyen Huy Duong[1]

[1]Institute of Biotechnology, Vietnam Academy of Science and Technology, 18 Hoang Quoc Viet, Ha Noi, Vietnam
[2]Graduate University of Science and Technology, Vietnam Academy of Science and Technology, 18 Hoang Quoc Viet, Ha Noi, Vietnam

Received 29 July 2024; accepted 19 March 2025

ABSTRACT

Apoptosis plays a crucial role in the normal development and differentiation of multicellular organisms and is essential for embryogenesis, metamorphosis, and elimination of unwanted cells. Like mammalian cells, yeast cells have evolved a number of cellular surveillance mechanisms including DNA damage checkpoint, stimulation of DNA repair, tolerance of DNA damage, and initiation of apoptosis. In *Saccharomyces cerevisiae*, the *HAP4* gene encodes the Hap4 protein which is a subunit of the heme-activated, glucose-repressed Hap2p/3p/4p/5p complex. This complex plays a crucial role in controlling the TCA cycle, the mitochondrial electron transport chain, ATP production and mitochondria biogenesis. Thus, the purpose of this study is to investigate the role of the *HAP4* gene by using the BY4742 (wild type) and specific knock-out yeast strains (Δ*hap4*) to elucidate the role of this gene in mitochondrial function and respiration, ATP synthesis, and apoptosis in response to DNA damage triggered by methyl methanesulfonate (MMS) treatment. The findings suggested that the fully functional mitochondria enhanced oxygen consumption and mitochondrial activity, attenuated ROS accumulation, and enabled efficient electron transport and ATP synthesis. High mitochondrial activity is performed as a cellular protective mechanism against oxidative stress. In contrast, deletion of the *HAP4* gene (Δ*hap4*), the main regulatory gene for the expression of respiratory proteins, caused a block of the electron transport chain, persistent inhibition of mitochondrial activity, thereby leading to a reduction of oxygen consumption. Low mitochondrial activity resulted in the development of oxidative stress, enhancement of sensitivity to DNA damaging agents. High intracellular ROS levels in Δ*hap4* cells posed a significant threat to mitochondrial DNA damage, impairment of mitochondrial respiration, inhibition of glycolytic enzymes (GAPDH, PYK), repression of ATP synthesis, and subsequent induction of cell death (apoptosis).

Keywords: apoptosis, DNA damage, *HAP4*, mitochondria, ROS, yeast.

Citation: Bui Van Ngoc, Nguyen Huy Duong, 2025. Role of yeast *HAP4* gene in mitochondrial function, oxidative phosphorylation, and apoptosis in response to DNA damage. *Academia Journal of Biology*, 47(1): 121–135. https://doi.org/10.15625/2615-9023/21232

[*]*Corresponding author email*: bui@ibt.ac.vn

INTRODUCTION

Within the mitochondrial electron transport chain (mtETC), about 1–2% of oxygen, rather than being reduced to H_2O, is partially reduced to the superoxide anion radical ($*O_2^-$). This unstable superoxide is converted into toxic hydrogen peroxide (H_2O_2) and then to hydroxyl free radicals (*OH) (Whalley et al., 2018). During oxidative phosphorylation, electrons are delivered through the mitochondrial respiratory complexes, and a proton gradient is established across the inner mitochondrial membrane as an energy source for ATP production. One important biochemical event associated with this metabolic process is the production of $*O_2^-$. When an electron escapes from the mtETC, especially at complex I (NADH-CoQ reductase) or III (CoQH2–cytochrome c reductase), it may react with molecular oxygen to form $*O_2^-$ that combines with a hydrogen atom yielding hydroperoxyl radical HO_2* (pKa = 4.88) (Whalley et al., 2018). Thus, at physiological pH, HO_2* exists as H_2O_2. $*O_2^-$ is constantly generated during cellular metabolism and can be converted to H_2O_2 and other reactive oxygen species (ROS) which cause cellular oxidative stress (Gomes & Juneau, 2016).

Apoptosis (programmed cell death) plays a crucial role in the normal development and differentiation of multicellular organisms and is essential for embryogenesis and metamorphosis (Krasovec et al., 2021). Apoptosis may be triggered by an external signal, acting at a receptor in the plasma membrane, or by internal events, e.g. viral infection (Zhang et al., 2023). In mammalian cells, apoptosis is also induced by a variety of agents such as heat shock (Kassis et al., 2021) and various cytotoxic substances (Kassis et al., 2021). Under either physiological or pathological conditions, apoptosis is mostly driven by interactions among several families of proteins, i.e. caspases, Bcl-2 family proteins, and inhibitors of apoptosis proteins (IAP proteins).

Like mammalian cells, yeast cells can undergo cell death accompanied by cellular markers of apoptosis. Cell death with apoptosis-like features has also been reported in yeast after treatment with acetic acid, UV-irradiation, glutathione-depleting chemicals and H_2O_2 (Lee et al., 2017; Mentel et al., 2023; Fang et al., 2024). The common denominator in most of these cell-death models that involve yeast seems to be an accumulation of ROS.

The *HAP4* gene encodes the Hap4 protein that is a subunit of the heme-activated, glucose-repressed Hap2p/3p/4p/5p complex (Carrillo-Garmendia et al., 2022). This complex acts as a transcriptional activator and global regulator of respiratory gene expression and plays a role in the transcription of genes involved in the TCA cycle, the mitochondrial electron transport chain, ATP production and mitochondria biogenesis (Capps et al., 2022). Thus, Hap4 plays a crucial role in controlling oxygen consumption and mitochondrial activity; and deletion of *HAP4* should result in the reduction of mitochondrial activity and oxygen consumption. Moreover, the expression of Hap4 is also repressed via the Mig1 pathway. Mig1 encoded by *MIG1* is a transcription factor involved in glucose repression. In high glucose conditions, the Hxk2/Snf1 complex binds to Mig1 to form a new complex that translocates from the cytoplasm to the nucleus to repress transcription of target genes encoding the utilization of sugars (Carrillo-Garmendia et al., 2022). Thereby, the activation of respiration is prevented in high glucose conditions (Carrillo-Garmendia et al., 2022; Lesko et al., 2023).

Thus, the aim of this study is to examine the role of the *HAP4* gene involved in mitochondrial function, the activity of glycolytic enzymes in energy production, and the regulation of yeast apoptosis in response to DNA damage upon treatment with genotoxic chemicals. By using the model yeast strain BY4742 (wild type) and the mutant Δ*hap4* defective in the *HAP4* gene, the role of the respective gene would be elucidated.

MATERIALS AND METHODS

Strains, media and growth conditions

Two yeast strains *Saccharomyces cerevisiae* used in this study are BY4742 wild type (Accession number: Y10000; Genotype:

MATα; his3Δ1; leu2Δ0; lys2Δ0; ura3Δ0; Source: EUROSCARF) and the mutant Δ*hap4* (Accession number: Y14959; Genotype: *MATα; his3Δ1; leu2Δ0; lys2Δ0; ura3Δ0; YKL109w::kanMX4*; Source: EUROSCARF). YPD (Yeast Peptone Dextrose) medium contains 10 g/L yeast extract, 20 g/L bacto peptone, and 20 g/L glucose. Cell growth was followed by optical absorbance measurement at 600 nm (OD_{600}). For treatment with DNA-damaging agents, e.g. methyl methanesulfonate (MMS), the medium was inoculated with overnight preculture and grown at 30 ºC to the mid-log phase (OD_{600} 0.6–0.8). Then, cultures were either nontreated (control) or treated with different concentrations of MMS (Sigma-Aldrich). Yeast cells were first inoculated in YPD medium, incubated at 30 ºC/250 rpm/overnight (pre-culture), then pre-culture was transferred in fresh respective media YPD (main culture).

OxoPlate® Assay

OxoPlate® (PreSens, Germany) was used to monitor oxygen consumption of cell growth in a medium. Oxygen consumption (%) and cell growth (OD_{600}) were monitored in 96-well OxoPlate® with round bottom integrated optical oxygen sensors, in which each well contained 75 µL of adjusted main culture (0.1 OD_{600}) and 75 µL of MMS with investigated concentration (i.e. 150 µL total).

The OxoPlate® was sealed with a breathable membrane (Diversified Biotech, USA), then introduced to Tecan Safire^2 Reader (Tecan, Switzerland) to measure fluorescence intensity at 540/650 nm (for indicator dye, $I_{indicator}$) and 540/590 nm (for reference dye, $I_{reference}$), and at 600 nm (for optical density of culture, OD_{600}). The measurement was carried out continuously over 18 hours with a kinetic interval of 30 min at 30 ºC. The calibration of the fluorescence reader was performed using a two-point calibration curve with oxygen free water (80 mM Na_2SO_3, *Cal 0*) and air-saturated water (*Cal 100*). The partial pressure of oxygen was calculated from the calibration curve.

Analysis of ROS level, mitochondrial features, and apoptosis by flow cytometry

Preparation: The main culture was split in two, one half culture as control (non-treated), another one was treated with 0.03% MMS. Aliquots (ca 50–100 µL) were taken at 3, 6, 8 and 24 h after MMS treatment and mixed with ca 900 µL PBS (ca 1 mL total). Aliquots were either stained with 50 µM dihydroethidium (DHE, Molecular Probes, in final concentration - in f.c) for ROS detection or stained with 1 µM MitoTracker® Green FM (Molecular Probes - in f.c) plus 5 µg/mL of propidium iodide (PI, Sigma-Aldrich, in f.c) for mitochondrial activity detection. For cell cycle analysis, after centrifugation, the pellets were fixed in 70% ethanol at 4 ºC for 24 hours, washed twice with ice-cold PBS and resuspended in 500 µL PBS. Cell suspensions were incubated with RNase A (50 µg/mL) for 30 min at 37 ºC and sequentially stained with cold PI solution (50 µg/mL) in the dark for 1 h (Bui et al., 2024).

Flow cytometry analysis (FACS): FACS® Calibur (Becton Dickinson) and CellQuest Pro analysis software were used to quantified the fluorescence intensity of DHE (excitation and emission wavelength at 488 and 564–606 nm, FL2 filter), MitoTracker® and NAO (excitation and emission wavelength at 488 and 525–550 nm, FL1 filter) for determination of ROS level, mitochondrial activity, and mitochondrial biogenesis, respectively. The analyzed fluorescence signal was given in the mean value of fluorescence intensity at the indicated time point (time course). The final graph performs overlapping histograms of fluorescence intensity against relative cell number according to time course. For apoptosis analysis, the annexin V/PI staining assay (BD Biosciences, Germany) was used to analyze cell apoptosis according to the protocol described in our previous study (Bui et al., 2024). In brief, living cells were determined as cells negative for both V and PI (V−/PI−), early apoptosis as cells positive for annexin V but negative for PI (V+/PI−), late apoptosis as cells positive for both annexin V and PI (V+/PI+), and necrotic cells as cells

negative for V but positive for PI (V−/PI+). All assays and measurements were performed at least 3 times for reproducibility.

Enzymatic Assay

Enzymatic Assay was used to determine the activity of glycolytic enzymes. In this research, it was applied to determine two Michaelis Menten constants, such as V_{max} and K_m of glycealdehyde-3-phosphate dehydrogenase (GAPDH, EC 1.2.1.12) and pyruvate kinase (PYK, EC 2.7.1.40).

Protein isolation: The main culture was divided in two, one half culture as control (non-treated), another one was treated with 0.03% MMS. Aliquots (ca 20 OD_{600} units of cells) were taken at 4 hours and 24 hours, centrifuged at 7000 rpm/4 ºC/3 min. Pellets were resuspended with 1 g glass beads and 500 µL of Extraction Buffer (20 mM Hepes pH 7.1, 100 mM KCl, 5 mM EDTA pH 8, 1 mM DTT, and 0.1% Tween). Samples were vortexed 2 × 5 min with cooling on ice in between, freezed at -20 ºC/overnight, and 1 × 5 min in Mixer Mill MMS 300 (Retsch). Broken cell suspensions were centrifuged at 13,000 rpm/4 ºC/20 min, supernatants (cell lysates) were immediately used for Enzymatic Assay to determine individual enzyme activity (V_{max}) and K_m, concomitantly used for determination of protein content by Bradford method.

Assay execution: The method followed the protocol as described in our previous reports (Kitanovic et al., 2009; Bonowski et al., 2010). Briefly, GAPDH activity was measured at 30 ºC by coupling the production of glycerate-1,3-diphosphate from 3-phosphoglyceric acid to the consumption of NADH, using a spectrophotometric assay in a coupled 3-phosphoglyceric phosphokinase-GAPDH system. PYK activity was measured at 30 ºC by coupling the production of pyruvate from phospho(enol)-pyruvate and ADP to the consumption of NADH, using a spectrophotometric assay in a coupled PYK-lactic dehydrogenase system. The reactions were initiated by the addition of crude extract and were followed by a decrease in A_{340} nm.

Data analysis: V_{max} and K_m were determined from enzyme activities at different substrate concentrations [*S*]. R function *nls* (nonlinear least squares) was used to perform a direct nonlinear regression of the Michaelis Menten formula to determine these constants (Bonowski et al., 2010). The data were then saved in RData files and analyzed by R program. The final results were plotted in R graphs that represent the kinetic curves of Michaelis Menten constants performing the relationship between V_{max} and K_m values. Finally, V_{max} and K_m values were represented in bar diagrams.

Analysis of ATP content by High Performance Ion Exchange Chromatography (HPIC)

Metabolite extraction and sample preparation: The sampling preparation was described previously (Loret et al., 2007). Briefly, 20 units OD_{600} of cell culture were withdrawn at the indicated time point, rapidly collected by vacuum filtration (Glass Filter, Millipore™) through a Sartolon polyamide membrane (Sartorius, Germany). The cell-adherent membrane was quenched in 5 mL buffered ethanol (75% ethanol, 10 mM Hepes, pH 7.1) in a 50 mL-glass tube (Lenz, Laborglas- instruments, Germany), shortly vortexed, incubated at 85 ºC/4 min in water bath, and immediately put on ice. The membrane was then washed 2 × 0.5 mL with absolute ethanol to rinse the rest on the membrane in the solvent. The solvent containing cell extract suspension was evaporated to dryness at 35–40 ºC under a vacuum rotary around 35–50 mbar (Büchi, Rotavapor R, Switzerland). Cell extract was resuspended in 0.5 mL deionized water, centrifuged at 13,000 rpm/4 ºC/5 min. The supernatant was introduced to HPIC for analysis.

Analysis of nucleotide content: Supernatants (ca 200 µL) were transferred into 1.5 mL-screw thread vials with glass inserts (VWR™) and analyzed by High Performance Ion Exchange Chromatography (HPIC, Dionex - ICS - 3000, USA) equipped with gradient pump and conductivity detector

along with UV detector (wavelength was set either to 220 or 260 nm). For the chromatographic separation, an AG11 guard column (50 mm × 2 mm i.d.) and 2 AS11 analytical columns (250 mm × 2 mm i.d.) (Dionex) in series were used. A flow of 0.35 ml/min was maintained throughout all runs. The suppressor current was set to 70 mA. The sample injection volume was 5 µL. The data was analyzed by Chromeleon software (Dionex, ICS - U3000). The content of metabolite (ATP) was then quantified by Chromeleon software based on the calibration curve and calculated in µmol/g DW (dry weight). The analytical protocol follows the method described by Ritter (2006) (Ritter et al., 2006).

RESULTS AND DISCUSSION

In yeast, the recovery of mitochondrial function and respiration as well as the increase of cell growth depend on the activity of some key genes. One of which is the *HAP4* gene that plays an important role in the mitochondrial electron transport chain (mtETC), mitochondrial activity, and apoptosis (Leadsham & Gourlay, 2010; Kawai et al., 2019; Capps et al., 2022). Thus, the accelerated oxygen consumption could depend on the activation of genes regulating mitochondrial and respiratory activity (*HAP4*).

Role of *HAP4* in mitochondrial features and respiration in response to DNA damage

The results illustrated in Figure 1 indicate that treatment with a genotoxic chemical (MMS) affects the mitochondrial respiration of cells, especially mutant cells (Δ*hap4*) leading to reduced oxygen consumption and cell proliferation. The effect of DNA damage induced by MMS treatment on oxygen consumption and cell growth was a concentration-dependent inhibition, i.e. the higher the MMS concentration, the more inhibition and vice versa (Fig. 1).

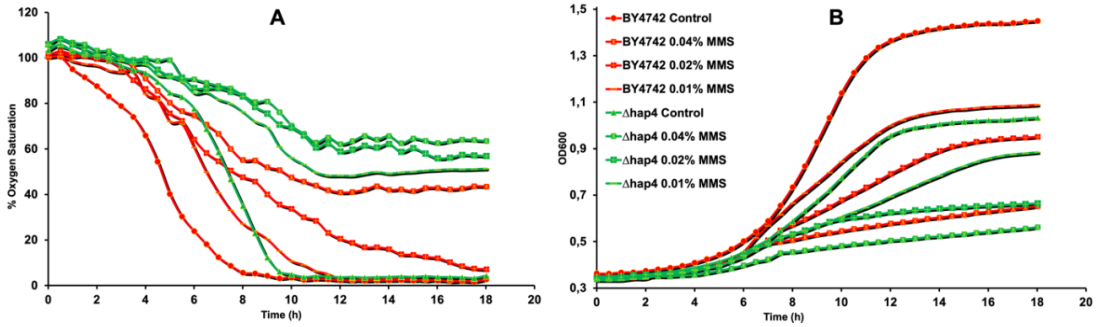

Figure 1. The kinetic of oxygen consumption (A) and cell growth (B) of BY4742 wild type and the Δ*hap4* mutant upon treatment with MMS. The standard deviations of measurements were less than 5%, thus omitted. The legends in the growth curves (B) are also ones in the kinetic of oxygen consumption (A)

Wild type BY4742 cells were less susceptible to MMS than mutant Δ*hap4* cells. Indeed, cells lacking the *HAP4* gene consumed up to 50% of oxygen in the medium upon treatment with 0.01–0.04% MMS (green lines, Fig. 1A), while the wild type consumed approximately 50% of oxygen even treated with the highest MMS concentration (0.04%) and was able to regain mitochondrial respiration and continue oxygen consumption at lower treated MMS concentrations until oxygen depleted (red lines, Fig. 1A). Thus, wild type cells were able to withstand these stress conditions, subsequently regaining mitochondrial function and overcoming inhibition of oxygen usage and cell growth better than mutant cells (Fig. 1).

As compared with wild type cells, treatment with different MMS concentrations more strongly inhibited, or totally blocked, mitochondrial functions of the mutant cells

leading to slower or no oxygen consumption followed by inhibition of cell growth. Mitochondrial functions only recovered by accelerated oxygen consumption until depletion in the medium when exposed to lower concentrations of MMS (Fig. 1).

Indeed, the *HAP4* gene controls the heme-activated and glucose repressed Hap2p/3p/4p/5p complex that plays a crucial role in the transcription of genes involved in the TCA cycle and mtETC (Capps et al., 2022; Carrillo-Garmendia et al., 2022). Deletion of the *HAP4* gene (Δ*hap4*) caused strong suppression of oxygen consumption and cell growth even upon treatment with lower doses of genotoxic chemicals (Fig. 1). The oxygen consumption could depend on mitochondrial and respiratory activity. The further experiments were, therefore, continued on mitochondrial features and respiration, namely ATP synthesis.

Changes in mitochondrial features in response to DNA damage

Besides the central role of mitochondria in ATP production, mitochondria also play a crucial role in oxidative stress and DNA damage response as well as apoptosis and cancer (Liu et al., 2023). Additionally, mitochondria also produce considerable quantities of superoxide ($^*O_2^-$) and hydrogen peroxide (H_2O_2) that in conjunction with its large iron stores can lead to mitochondrial DNA damage (Shokolenko et al., 2009; Senoo et al., 2016; Stenberg et al., 2022). Mitochondrial DNA (mtDNA) might be more prone to oxidative damage than nuclear DNA (nDNA) (Yakes & Van Houten, 1997; Rong et al., 2021).

In general, mitochondrial activity of all control and MMS-treated cultures gradually decreased over the cultivation time. In particular, it started to decrease at the beginning of cultivation, increase slightly higher at around 8 hours, and started to decrease again up to 24 hours (Fig. 2). This effect could be explained that when glucose was available in full medium (YPD) within 3 h, fermentation rather than respiration was preferred, resulting in low mitochondrial activity. When glucose was completely exhausted at around 6–8 hours of cultivation, respiration was preferred, and subsequently mitochondrial activity increased. Additionally, the mitochondrial activity of all MMS-treated cells decreased faster than in controls: the lower measured fluorescence intensity is the result of impairment of mitochondrial function upon MMS treatment (Fig. 2).

Moreover, the high mitochondrial activity of the BY4742 wild type was able to recover mitochondrial function regain oxygen consumption faster and increase cell survival better than the Δ*hap4* mutant. The Δ*hap4* mutant was not able to regain mitochondrial function, resume oxygen consumption and continue cell proliferation when exposed to stress conditions including treatment with genotoxic chemicals as the wild type could.

Thus, disruption of the *HAP4* gene controlling the heme-activated, glucose-repressed Hap2p/3p/4p/5p complex strongly enhanced the inhibition of the MMS-mediated mitochondrial activity as compared with the wild type.

It might be that the decreased mitochondrial function and oxygen consumption probably result from mitochondrial DNA (mtDNA) damage triggered by MMS treatment that induces high ROS accumulation and further impair mtETC or mitochondrial activity. Because mtDNA seems to be a critical target for such oxidative damage and is particularly susceptible to ROS generated by the mitochondrial electron transport chain due to its close proximity (Shokolenko et al., 2009; Cui et al., 2012; Stenberg et al., 2022). Consequently, the ROS level was further determined.

As shown in Figure 3, the ROS level of all MMS-treated cells gradually increased throughout the cultivation period. However, ROS levels of control cells dramatically increased at around 6–8 hours during the log-phase, reaching a maximum at 8 hour, then starting to decrease in the stationary phase as glucose in the medium is completely exhausted. Cells lacking *HAP4* (Δ*hap4)* yield high ROS levels in the control culture, particularly in the MMS-treated culture, during

mid-log and log phases (6–8 hours) as compared with the wild type (Fig. 3).

One explanation could be that ROS are generated during normal metabolism and proportional to increased oxygen consumption, i.e. high mitochondrial activity and high growth rate. Also, mitochondria are a source of cellular ROS as a result of electron leakage from mtETC. Leaked electrons could react with molecular oxygen to form $*O_2^-$ which is then converted to H_2O_2 at physiological pH. Thus, electron leakage capacity correlates with mtETC activity (Gomes & Juneau, 2016; Whalley et al., 2018).

As mentioned above, mtDNA suffers more damage than nuclear DNA (nDNA) and is susceptible to ROS generated by the mtECT. Certainly, high ROS accumulation and H_2O_2 concentration at physiological pH caused damage to mtDNA and mitochondria activity.

Next, further experiments were continued to verify the correlation between mitochondrial activity and mitochondrial biogenesis or mitochondrial copy number. Mitochondrial biogenesis is the process by which new mitochondria are formed in the cell. Mitochondrial biogenesis is activated by numerous different signals during times of cellular stress or in response to environmental stimuli. It is thought that a higher mitochondrial copy number (or higher mitochondrial mass) is protective for the cell. Mitochondrial biogenesis was reported to increase in response to DNA damage (Fu et al., 2008; Callender et al., 2021). DNA double-strand breaks (DSBs) have been reported to upregulate the abundance of mitochondria (Garcia et al., 2017; Dahal et al., 2018; Nadalutti et al., 2020). MMS is an alkylating agent and carcinogen, it methylates N^7-deoxyguanine and N^3-deoxyadenine bases of DNA, it is known to directly cause DNA double-strand breaks and stall replication forks in *S. cerevisiae* (Yang et al., 2010).

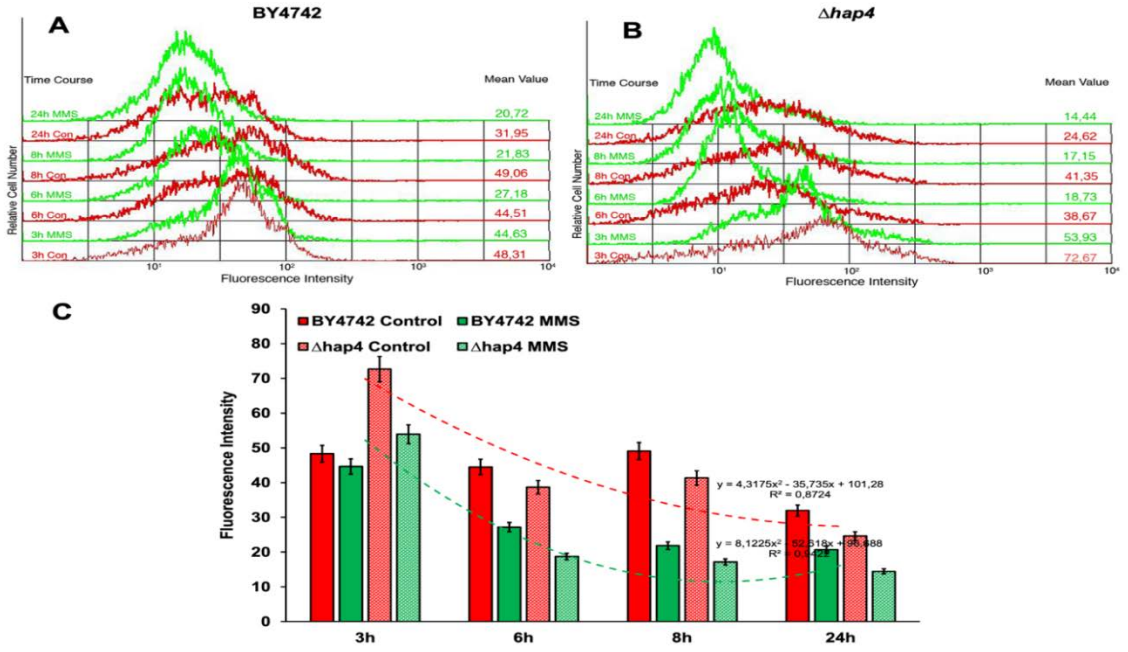

Figure 2. Modulation of mitochondrial activity of BY4742 (A) and Δ*hap4* (B) in response to DNA damage. Fluorescence intensity was quantified and analyzed by FACS for measuring mitochondrial activity, results are given as mean value. Graphs represent mean value of fluorescence intensity measured at each time point when aliquots were taken. The dash lines with quadratic equations represent the trends of mitochondrial activity during 24 hours of cultivation (C)

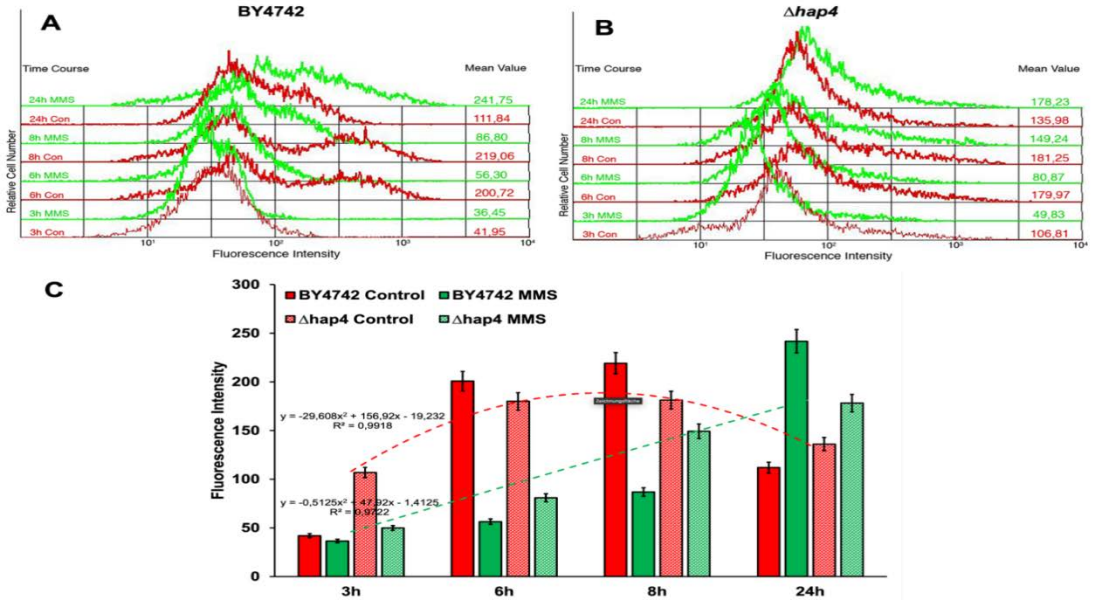

Figure 3. ROS accumulation of BY4742 (A) and Δ*hap4* (B) in response to DNA damage. Fluorescence intensity was quantified and analyzed by FACS for determining ROS level, results are given as mean value. Graphs represent mean value of fluorescence intensity measured at each time point when aliquots were taken. The dash lines with quadratic equations represent the trends of ROS accumulation during 24 hours of cultivation (C)

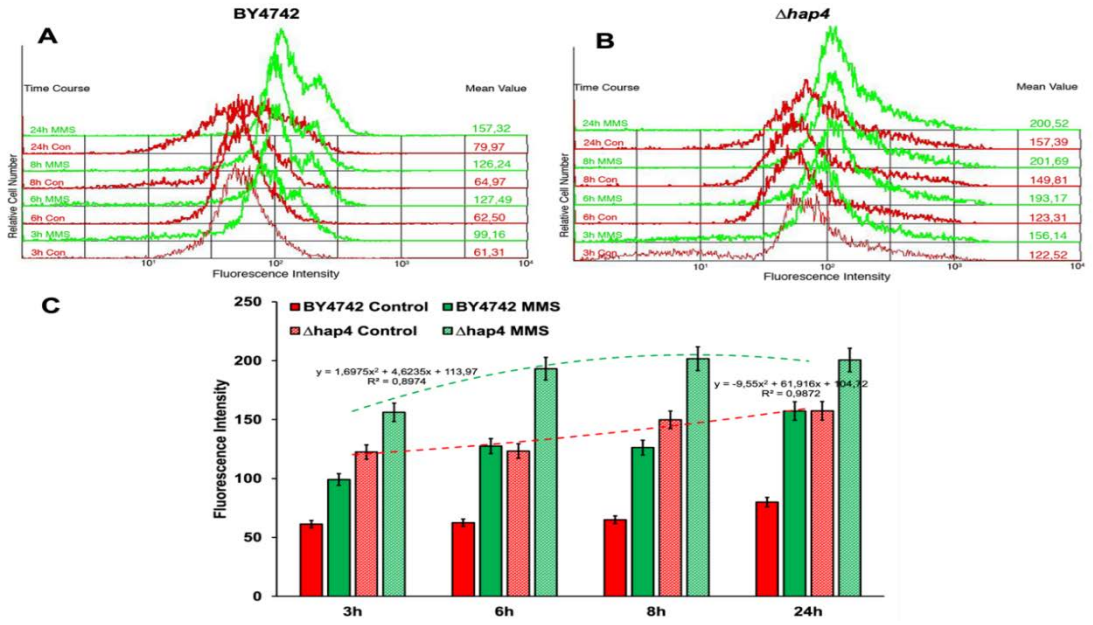

Figure 4. Modulation of mitochondrial biogenesis of BY4742 (A) and Δ*hap4* (B) in response to DNA damage. Fluorescence intensity was quantified and analyzed by FACS for determining mitochondrial biogenesis, results are given as mean value. Graphs represent mean value of fluorescence intensity measured at each time point aliquots were taken. The dash lines with quadratic equations represent the trends of mitochondrial biogenesis during 24 h of cultivation (C)

The findings indicate that mitochondrial activity (Fig. 2) gradually decreased in control cultures, but mitochondrial biogenesis (Fig. 4) gradually increased during cultivation. Similarly, MMS-treated cells showed a decrease of mitochondrial activity (Fig. 2), but an increase of mitochondrial biogenesis (Fig. 4) which occurred more rapidly and more intensively than the control cells as a result of high ROS accumulation triggered by MMS treatment (Fig. 3). In other words, mitochondrial biogenesis in all control conditions also increased but was much slower than in MMS-treated cultures. DNA damage reduced mitochondrial activity, but induced mitochondrial biogenesis - new mitochondria were formed. This effect seems to be a protective mechanism for the cells.

Thus, the mutant Δ*hap4* triggered intensively mitochondrial biogenesis (high mitochondrial mass) upon either control or MMS treatment as compared with all cells. This effect could be explained that high mitochondrial biogenesis is not directly controlled by Hap4p, but probably by other components of the Hap2p/3p/4p/5p complex. This complex controls the transcription of genes involved in the TCA cycle, mtETC, and mitochondria biogenesis (Kawai et al., 2019; Capps et al., 2022; Carrillo-Garmendia et al., 2022).

Effect of DNA damage on the activity of glycolytic enzymes

As mentioned, mitochondria are a source of ATP but also a major source of cellular ROS. When the ROS level reaches a certain threshold, it can damage mtDNA leading to inhibition of mitochondrial activity with a subsequent decrease of ATP synthesis. So, when the main energetic pathway is blocked, the carbohydrate flux could shunt into the upper or lower part (early or late stage) of glycolysis depending on the activity of glycolytic enzymes. Thus, investigations were continued on analysis of the activity of some key enzymes in glycolysis in response to DNA damage induced by MMS treatment.

The results showed that MMS treatment strongly reduced the GAPDH activity of all strains from as early as 4 hours up to 24 hours of treatment, especially the GAPDH activity all ceased after 24 hours of treatment (Fig. 5B). The mutant Δ*hap4* was more sensitive to MMS than the wild type (Figs. 5A, B). GAPDH (glycealdehyde-3-phosphate dehydrogenase, EC 1.2.1.12) is a central glycolytic enzyme, catalyzing the generation of 1,3-diphosphoglycerate from glyceraldehyde-3-phosphate in the sixth step of glycolysis, the process in which glucose is ultimately converted into pyruvate. GAPDH plays an important role in energy production (Cornett et al., 2022), in response to oxidative stress and in apoptosis (Dastoor and Dreyer, 2001; Nie et al., 2021). Our own previous research indicated that high ROS accumulation strongly inhibits GAPDH activity upon MMS treatment (Kitanovic et al., 2009). Thus, GAPDH is a preferred target for high ROS accumulation.

Similar to GAPDH, PYK activity of all strains was nearly inhibited after 4 h and strongly decreased after 24 hours of MMS treatment (Figure 5, C–D). Also, the PYK activity of the Δ*hap4* strain was comparatively lower than that of the wild type after 24 hours of MMS treatment.

PYK (pyruvate kinase, EC 2.7.1.40) catalyzes the final step of glycolysis, converting phospho-(enol)pyruvate and ADP into pyruvate and ATP. Once generated, pyruvate can enter mitochondria to fuel aerobic metabolism through oxidative phosphorylation or it can remain in the cytoplasm and be converted to acetate, ethanol (in yeast) or lactate (in mammals) via fermentation or anaerobic metabolism (Whalley et al., 2018). Our previous report also showed that PYK activity was strongly inhibited by high intracellular ROS levels due to MMS treatment (Kitanovic et al., 2009).

In addition, MMS treatment did not affect the affinity (K_m) of the individual enzymes GAPDH, PYK, and their specific substrates as compared to controls. Mostly, MMS reduced the affinity (increased K_m) of enzymes for

their substrates, in some cases they promoted affinity (decreased K_m). The inhibited activity of GAPDH and PYK upon MMS treatment - hence, raising the question as to the fate of the carbohydrate flux. Here it was supposed that DNA damage induced by MMS treatment causes a shift of metabolic flux to the early stage of glycolysis, namely the PPP, rather than to the late stage of glycolysis, namely the TCA cycle and oxidative phosphorylation. In other words, carbohydrate flux (glucose) does not enter the TCA cycle and oxidative phosphorylation that leads to a reduction of intracellular ATP level. To prove this assumption, the ATP level was analyzed by the HPIC method and represented in Figure 6.

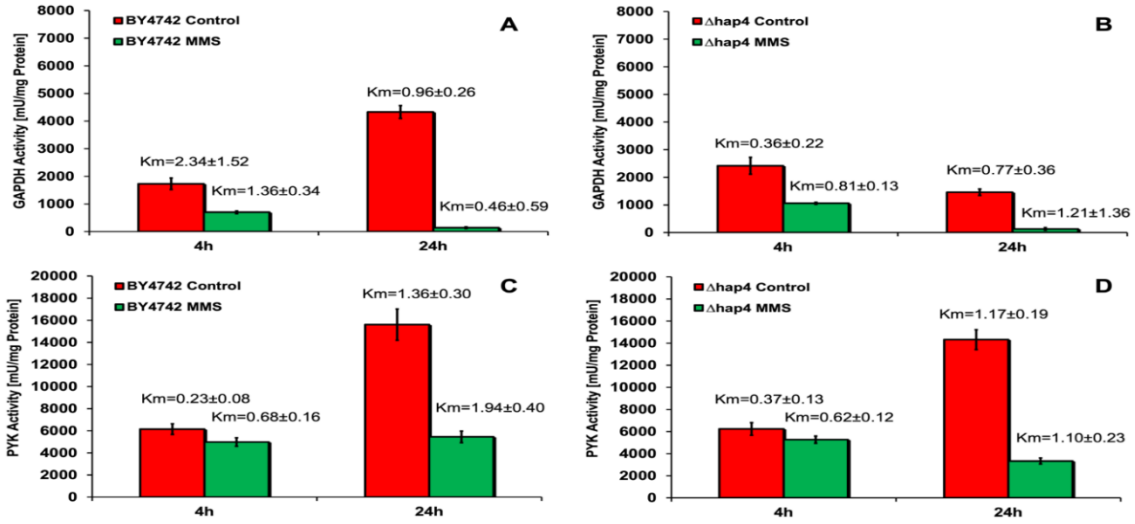

Figure 5. Changes in the activity of glycolytic enzymes of BY4742 and Δ*hap4* in response to DNA damage. Cell lysates were introduced to execute the Enzymatic Assay for the determination of Michaelis-Menten constants, V_{max} and K_m. Graphs represent the activity of GAPDH (A, B) and PYK (C, D) expressed by V_{max} in mU/mg protein and together with K_m in mM

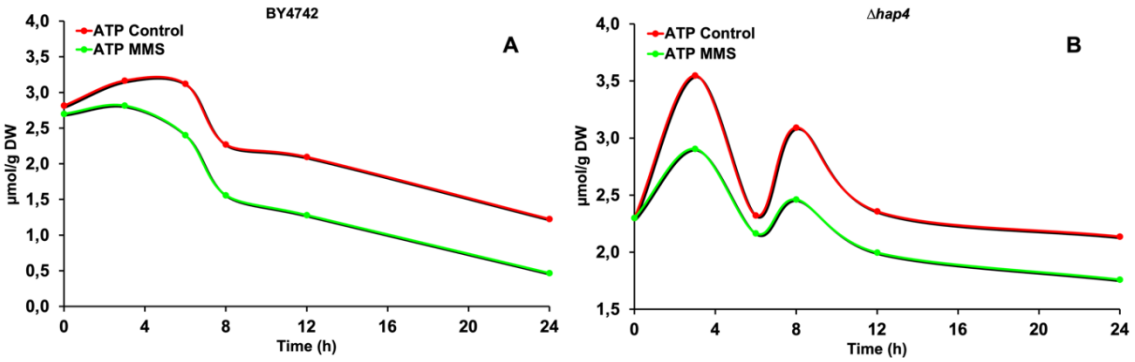

Figure 6. Changes in ATP levels of BY4742 (A) and Δ*hap4* (B) cells in response to DNA damage. Intracellular metabolite extracts were analyzed by HPIC to quantify the ATP concentration. The value of ATP levels was calculated in µmol/g DW (dry weight)

As assumed, MMS treatment suppressed ATP synthesis of both the BY4742 and Δ*hap4* already after 3 h of treatment resulting in the reduction of ATP levels as compared with the controls (Fig. 6). The ATP synthesis was inhibited as a result of impaired mitochondrial

activity (Fig. 2) and carbohydrate flux was re-routed towards the early stages of glycolysis leading to lower ATP levels. Thus, MMS-treated cells were not able to maintain their energy balance as compared to the controls.

Besides the central role of mitochondria in energy metabolism and the respiratory chain, mitochondria also play an important role in apoptosis (programmed cell death) (Van Houten et al., 2006; Guaragnella et al., 2014; Nadalutti et al., 2020). Furthermore, unregulated PKA activity can lead to the production of mitochondria that are prone to the production of ROS and apoptosis (Leadsham and Gourlay, 2010).

It is hypothesized that the reduction of mitochondrial activity and oxygen consumption under high oxidative stress (ROS) could lead to the induction of apoptosis cells that lack key genes involved in the control of apoptosis like *HAP4*. As expected, MMS treatment not only reduced the relative cell number, i.e. increased the percentage of apoptotic cells, but also caused an increase in the population of cells in early apoptosis (V+/PI–), late apoptosis (V+/PI+), and necrosis (V–/PI+) as compared with the controls (Fig. 7). In other words, the living cells gradually decreased, while the amount of early/late apoptotic and necrotic cells steadily increased. Moreover, the relative cell number of the Δ*hap4* lacking *HAP4* was more reduced than that of the wild type (Fig. 7).

Thus, mitochondria act as "executioners" in apoptosis. Enhancement of mtDNA repair should confer protection from cell death, whereas loss of mtDNA repair should promote cell death (Van Houten et al., 2006; Leadsham & Gourlay, 2010; Lee et al., 2017).

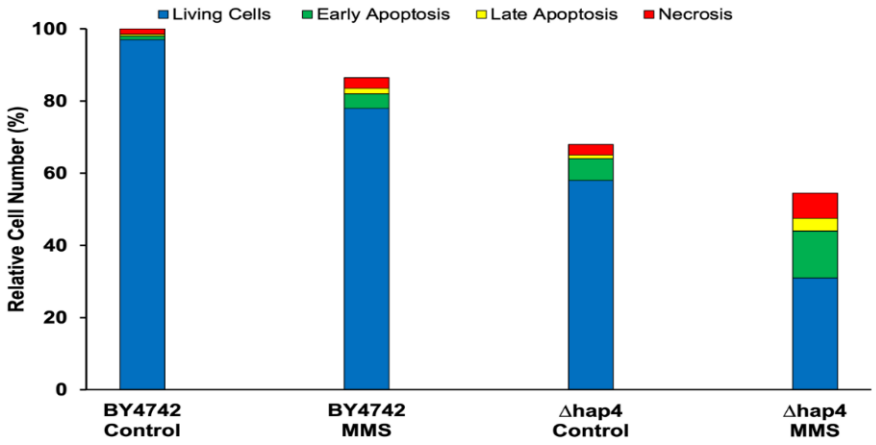

Figure 7. Induction of apoptosis in BY4742 and Δ*hap4* cells in response to DNA damage. Apoptosis stages and apoptotic cell ratios (%) were analyzed by flow cytometry (FACS) using annexin V/PI double staining and calculated by hemacytometer using trypan blue staining, respectively. All measurements were performed at least 3 times for reproducibility

As shown previously, DNA damage blocks the late stage of glycolysis as a result of inhibition of GAPDH and PYK activities, consequently inhibits ATP synthesis. The carbohydrate flux (glucose) does not enter the TCA cycle and mtETC to produce ATP. Probably, the carbohydrate flux diverts to the hexosamine biosynthesis pathway, pentose phosphate pathway, and glycogen and trehalose synthesis. To support these statements, additional investigations will be performed in our further work.

CONCLUSION

In general, the findings showed that DNA damage induced by MMS treatment strongly reduces mitochondrial activity and oxygen consumption in response to high ROS accumulation, but enhances mitochondrial biogenesis in which new mitochondria are

formed via the cellular protective response. High of ROS accumulation caused inhibition of glycolytic enzymes (GAPDH, PYK), decrease of ATP generation, and triggering of signals for cell death or apoptosis (Fig. 8). Thus, *Hap4* plays a crucial role in controlling oxygen consumption and mitochondrial activity; and deletion of *Hap4* should result in reduction of mitochondrial activity and oxygen consumption.

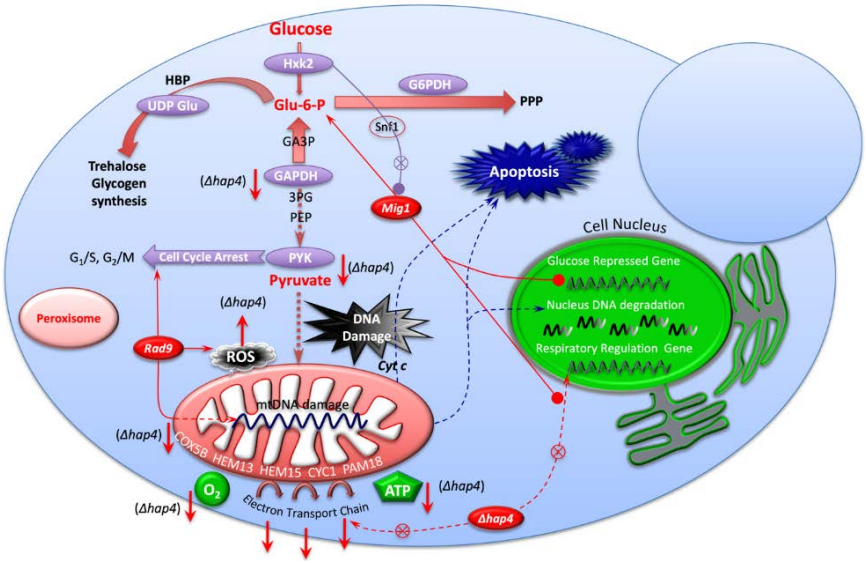

Figure 8. Schematic summary of the role of yeast *HAP4* gene in mitochondrial function, oxidative phosphorylation, and apoptosis in response to DNA damage. Treatment of DNA damage agents (MMS) strongly inhibits mitochondrial electron transport chain - mtETC (perhaps because of damaging mtDNA) and decreases oxygen consumption of the mutant Δ*hap4*. MMS treatment induced high ROS accumulation, especially in the mutant defective in the *HAP4* gene. High ROS directly inhibit GAPDH activity, this effect downstream reduces PYK activity leading to decreased mitochondrial activity and respiration. A further effect is the inhibition of ATP synthesis. Thus, glucose flux does not shunt to the TCA cycle and mtETC where a large amount of ATP molecules is produced. Furthermore, high ROS causes loss of cell viability and induction of apoptosis

Acknowledgements: We thank Stefan Wölfl, Ana Kitanovic for valuable comments regarding the experiments and for sharing ideas regarding data analysis. This work was supported by the SysMO Project Network (EU-BMBF) on Systems Biology of Microorganisms (MOSES, WP 4.3, S.W. and A.K.).

REFERENCES

Bonowski F., Kitanovic A., Ruoff P., Holzwarth J., Kitanovic I., Bui N., Lederer E., Wölfl S., 2010. Computer controlled automated assay for comprehensive studies of enzyme kinetic parameters. *PLoS ONE*, 5(5): e10727. https://doi.org/10.1371/journal.pone.0010727

Bui V. N., Nguyen T. P. T., Nguyen H. D., Phi Q. T., Nguyen T. N., Chu H. H., 2024. Bioactivity responses to changes in mucus-associated bacterial composition between healthy and bleached Porites lobata corals. *Journal of invertebrate pathology*, 206: 108164. United States. https://doi.org/10.1016/j.jip.2024.108164

Callender L. A., Schroth J., Carroll E. C., Garrod-Ketchley C., Romano L. E. L., Hendy E., Kelly A., Lavender P., Akbar A. N., Chapple J. P., Henson S. M., 2021. GATA3 induces mitochondrial biogenesis in primary human CD4+ T cells during DNA damage. *Nature Communications*,

12(1): 3379. https://doi.org/10.1038/s41467-021-23715-7

Capps D., Hunter A., Chiang M., Pracheil T., Liu Z., 2022. Ubiquitin-Conjugating Enzymes Ubc1 and Ubc4 Mediate the Turnover of Hap4., a Master Regulator of Mitochondrial Biogenesis in *Saccharomyces cerevisiae*. *Microorganisms*, 10(12): 2370. https://doi.org/10.3390/microorganisms10122370

Carrillo-Garmendia A., Martinez-Ortiz C., Martinez-Garfias J. G., Suarez-Sandoval S. E., González-Hernández J. C., Nava G. M., Dufoo-Hurtado M. D., Madrigal-Perez L. A., 2022. Snf1p/Hxk2p/Mig1p pathway regulates hexose transporters transcript levels., affecting the exponential growth and mitochondrial respiration of *Saccharomyces cerevisiae*. *Fungal Genetics and Biology*, 161: 103701. https://doi.org/10.1016/j.fgb.2022.103701

Cornett K., Puderbaugh A., Back O., Craven R., 2022. GAPDH in neuroblastoma: Functions in metabolism and survival. *Frontiers in Oncology*, 12: 979683. https://doi.org/10.3389/fonc.2022.979683

Cui H., Kong Y., Zhang H., 2012. Oxidative Stress., Mitochondrial Dysfunction., and Aging. *Journal of Signal Transduction*, 2012(1): 646354. https://doi.org/10.1155/2012/646354

Dahal S., Dubey S., Raghavan S. C., 2018. Homologous recombination-mediated repair of DNA double-strand breaks operates in mammalian mitochondria. *Cellular and Molecular Life Sciences*, 75(9): 1641–1655. https://doi.org/10.1007/s00018-017-2702-y

Dastoor Z., Dreyer J. L., 2001. Potential role of nuclear translocation of glyceraldehyde-3-phosphate dehydrogenase in apoptosis and oxidative stress. *Journal of Cell Science*, 114(9): 1643–1653. https://doi.org/10.1242/jcs.114.9.1643

Fang J., Zhou G., Zhao H., Xie D., Zhang J., Kües U., Xiao Y., Fang Z., Liu J., 2024. An apoptosis-inducing factor controls programmed cell death and laccase expression during fungal interactions. *Applied Microbiology and Biotechnology*, 108(1): 135. https://doi.org/10.1007/s00253-023-12988-1

Fu X., Wan S., Lyu Y. L., Liu L. F., Qi H., 2008. Etoposide induces ATM-dependent mitochondrial biogenesis through AMPK activation. *PLoS ONE*, 3(4): e2009. https://doi.org/10.1371/journal.pone.0002009

Garcia I., Jones E., Ramos M., Innis-Whitehouse W., Gilkerson R., 2017. The little big genome: The organization of mitochondrial DNA. *Frontiers in Bioscience - Landmark*, 22(4): 710–721. https://doi.org/10.2741/4511

Gomes M. P., Juneau P., 2016. Oxidative stress in duckweed (*Lemna minor* L.) induced by glyphosate: Is the mitochondrial electron transport chain a target of this herbicide? *Environmental Pollution*, 218: 402–409. https://doi.org/10.1016/j.envpol.2016.07.019

Guaragnella N., Palermo V., Galli A., Moro L., Mazzoni C., Giannattasio S., 2014. The expanding role of yeast in cancer research and diagnosis: Insights into the function of the oncosuppressors p53 and BRCA1/2. *FEMS Yeast Research*, 14(1): 2−16. https://doi.org/10.1111/1567-1364.12094

Van Houten B., Woshner V., Santos J. H., 2006. Role of mitochondrial DNA in toxic responses to oxidative stress. *DNA Repair*, 5(2): 145−152. https://doi.org/10.1016/j.dnarep.2005.03.002

Kassis S., Grondin M., Averill-Bates D. A., 2021. Heat shock increases levels of reactive oxygen species., autophagy and apoptosis. *Biochimica et Biophysica Acta - Molecular Cell Research*, 1868(3): 118924. https://doi.org/10.1016/j.bbamcr.2020.118924

Kawai K., Kanesaki Y., Yoshikawa H., Hirasawa T., 2019. Identification of metabolic engineering targets for

improving glycerol assimilation ability of *Saccharomyces cerevisiae* based on adaptive laboratory evolution and transcriptome analysis. *Journal of Bioscience and Bioengineering*, 128(2): 162−169. https://doi.org/10.1016/j.jbiosc.2019.02.001

Kitanovic A., Walther T., Loret M. O., Holzwarth J., Kitanovic I., Bonowski F., Bui N. Van., Francois J. M., Wölfl S., 2009. Metabolic response to MMS-mediated DNA damage in *Saccharomyces cerevisiae* is dependent on the glucose concentration in the medium. *FEMS Yeast Research*, 9(4): 535–551. https://doi.org/10.1111/j.1567-1364.2009.00505.x

Krasovec G., Pottin K., Rosello M., Quéinnec É., Chambon J. P., 2021. Apoptosis and cell proliferation during metamorphosis of the planula larva of *Clytia hemisphaerica* (Hydrozoa., Cnidaria). *Developmental Dynamics*, 250(12): 1739−1758. https://doi.org/10.1002/dvdy.376

Leadsham J. E., Gourlay C. W., 2010. CAMP/PKA signaling balances respiratory activity with mitochondria dependent apoptosis via transcriptional regulation. *BMC Cell Biology*, 11: 92. https://doi.org/10.1186/1471-2121-11-92

Lee J. Y., Jun D. Y., Park J. E., Kwon G. H., Kim J. S., Kim Y. H., 2017. Pro-apoptotic role of the human YPEL5 gene identified by functional complementation of a yeast moh1Δ mutation. *Journal of Microbiology and Biotechnology*, 27(3): 633−643. https://doi.org/10.4014/jmb.1610.10045

Lesko M. A., Chandrashekarappa D. G., Jordahl E. M., Oppenheimer K. G., Bowman R. W., Shang C., Durrant J. D., Schmidt M. C., O'Donnell A. F., 2023. Changing course: Glucose starvation drives nuclear accumulation of Hexokinase 2 in *S. cerevisiae*. *PLoS Genetics*, 19(5): e1010745. https://doi.org/10.1371/journal.pgen.1010745

Liu Y., Sun Y., Guo Y., Shi X., Chen X., Feng W., Wu L. L., Zhang J., Yu S., Wang Y., Shi Y., 2023. An Overview: The Diversified Role of Mitochondria in Cancer Metabolism. *International Journal of Biological Sciences*, 19(3): 897−915. https://doi.org/10.7150/ijbs.81609

Loret M. O., Pedersen L., François J., 2007. Revised procedures for yeast metabolites extraction: Application to a glucose pulse to carbon-limited yeast cultures., which reveals a transient activation of the purine salvage pathway. *Yeast*, 24(1): 47−60. https://doi.org/10.1002/yea.1435

Mentel M., Illová M., Krajčovičová V., Kroupová G., Mannová Z., Chovančíková P., Polčic P., 2023. Yeast Bax Inhibitor (Bxi1p/Ybh3p) Is Not Required for the Action of Bcl-2 Family Proteins on Cell Viability. *International Journal of Molecular Sciences*, 24(15): 12011. https://doi.org/10.3390/ijms241512011

Nadalutti C. A., Stefanick D. F., Zhao M. L., Horton J. K., Prasad R., Brooks A. M., Griffith J. D., Wilson S. H., 2020. Mitochondrial dysfunction and DNA damage accompany enhanced levels of formaldehyde in cultured primary human fibroblasts. *Scientific Reports*, 10(1): 5575. https://doi.org/10.1038/s41598-020-61477-2

Nie F., Yan J., Ling Y., Liu Z., Fu C., Li X., Qin Y., 2021. Effect of Shuangdan Mingmu capsule., a Chinese herbal formula., on oxidative stress-induced apoptosis of pericytes through PARP/GAPDH pathway. *BMC Complementary Medicine and Therapies*, 21(1): 118. https://doi.org/10.1186/s12906-021-03238-w

Ritter J. B., Genzel Y., Reichl U., 2006. High-performance anion-exchange chromatography using on-line electrolytic eluent generation for the determination of more than 25 intermediates from energy metabolism of mammalian cells in culture. *Journal of Chromatography B: Analytical Technologies in the Biomedical and Life Sciences*, 843(2): 216–226. https://doi.org/10.1016/j.jchromb.2006.06.004

Rong Z., Tu P., Xu P., Sun Y., Yu F., Tu N., Guo L., Yang Y., 2021. The Mitochondrial Response to DNA Damage. *Frontiers in cell and developmental biology*, 9: 669379. https://doi.org/10.3389/fcell.2021.669379

Senoo T., Yamanaka M., Nakamura A., Terashita T., Kawano S., Ikeda S., 2016. Quantitative PCR for detection of DNA damage in mitochondrial DNA of the fission yeast *Schizosaccharomyces pombe*. *Journal of Microbiological Methods*, 127: 77−81. https://doi.org/10.1016/j.mimet.2016.05.023

Shokolenko I., Venediktova N., Bochkareva A., Wilson G. I., Alexeyev M. F., 2009. Oxidative stress induces degradation of mitochondrial DNA. *Nucleic Acids Research*, 37(8): 2539−2548. https://doi.org/10.1093/nar/gkp100

Stenberg S., Li J., Gjuvsland A. B., Persson K., Demitz-Helin E., Gonzalez-Pena C., Yue J. X., Gilchrist C., Ärengård T., Ghiaci P., Larsson-Berglund L., Zackrisson M., Smits S., Hallin J., Höög L. L., Molin M., Liti G., Omholt S. W., Warringer J., 2022. Genetically controlled mtDNA deletions prevent ROS damage by arresting oxidative phosphorylation. *eLife*, 8(11): e76095. https://doi.org/10.7554/elife.76095

Whalley N. A., Walters S., Hammond K., 2018. Molecular Cell Biology. *Molecular Medicine for Clinicians*: 37−49. https://doi.org/10.18772/22008014655.9

Yakes F. M., Van Houten B. 1997., Mitochondrial DNA damage is more extensive and persists longer than nuclear DNA damage in human cells following oxidative stress. *Proceedings of the National Academy of Sciences of the United States of America*, 94(2): 514−519. https://doi.org/10.1073/pnas.94.2.514

Yang Y., Gordenin D. A., Resnick M. A., 2010., A single-strand specific lesion drives MMS-induced hyper-mutability at a double-strand break in yeast. *DNA Repair*, 9(8): 914−921. https://doi.org/10.1016/j.dnarep.2010.06.005

Zhang Y., Li B. X., Mao Q. Z., Zhuo J. C., Huang H. J., Lu J. B., Zhang C. X., Li J. M., Chen J. P., Lu G., 2023. The JAK-STAT pathway promotes persistent viral infection by activating apoptosis in insect vectors. *PLoS Pathogens*, 19(3): e1011266. https://doi.org/10.1371/journal.ppat.1011266